p$\bar{p}$ Note 20

C. Rubbia
July 11, 1977

EUROPEAN ORGANIZATION FOR NUCLEAR RESEARCH

AN INTEGRATED MAGNET AND IMPACTOMETER ARRANGEMENT

C. Rubbia

Abstract

The variety of events which almost certainly will occur at p$\bar{p}$ collider energies suggest the simultaneous presence of a magnetic and calorimetric analyses. The possibility of an integrated magnet-calorimeter structure is discussed in which ionisation sampling elements are inbedded in the superconductor-stabilising structure at liquid Helium temperature. The massive hadron absorber plates mantain also the huge mechanical forces produced by the currents. A possible geometry for a cosθ current distribution generating a dipole field is discussed. The properties of the sampling counters at liquid Helium temperature are reviewed.

1. How to sample $\frac{dE}{dX}$ at liquid Helium temperature?

Liquid Argon[1] is now almost universally used as a sampling medium for counters for photon and hadron showers. Its properties, i.e. the large density, low cost and relatively high liquification temperature make it ideal in the majority of applications. In our case however the Argon will be a frozen solid. Electrons can be easily extracted from solid Argon and indeed the drift velocity is somewhat higher than in the case of a liquid (see Fig. 1). However polarization effects almost inevitably occur and there is no known trick to remove these effects. Hence in a matter of minutes the detector will stop working.

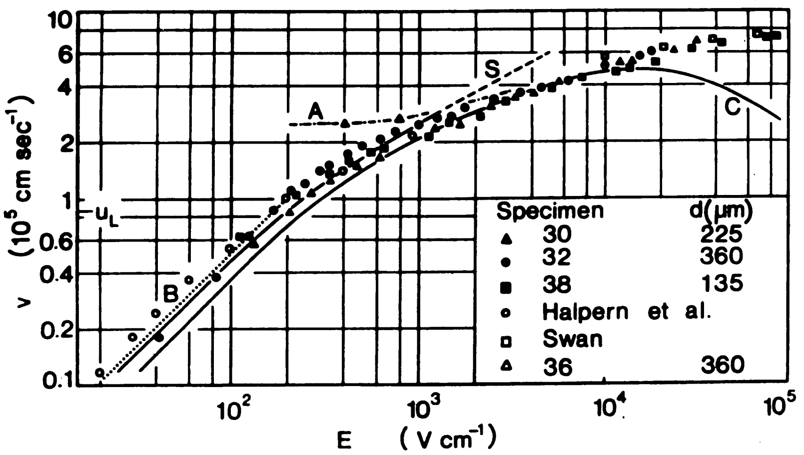

a)

Fig.1a) The field dependence of the electron drift velocity in liquid Ar at 85 K.

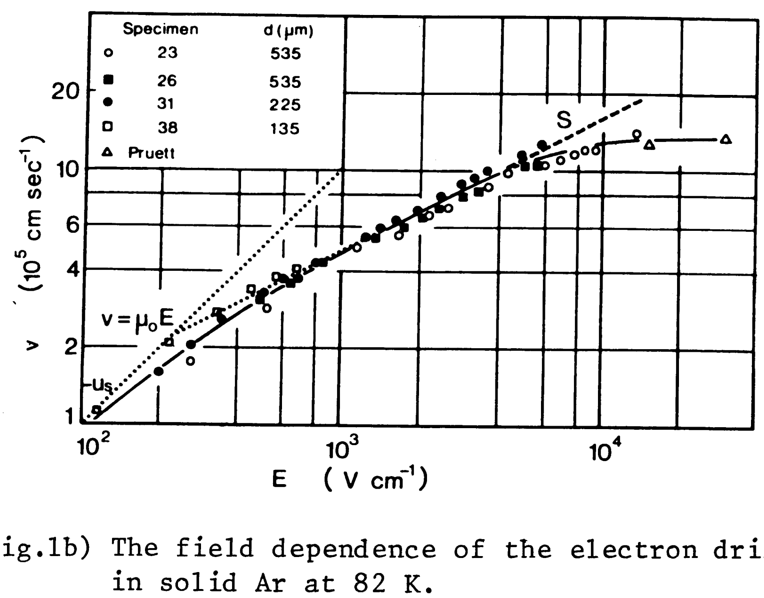

b)

Fig.1b) The field dependence of the electron drift velocity in solid Ar at 82 K.

Another a priori possibility is the one of using liquid Helium of sufficient purity to collect the electrons produced by the ionizing particles traversing it. However a dramatic drop in the electron mobility μ is observed at low temperatures and even at moderate densities[2)] (Fig. 2). A model which fits the experimental observation is one in which a microbubble is formed around the electron thus reducing the mobility. Similar bubble effect have been observed in H_2 and Neon close to their triple point[3)]. Therefore a liquid Helium calorimeter is again excluded by this phenomenon.

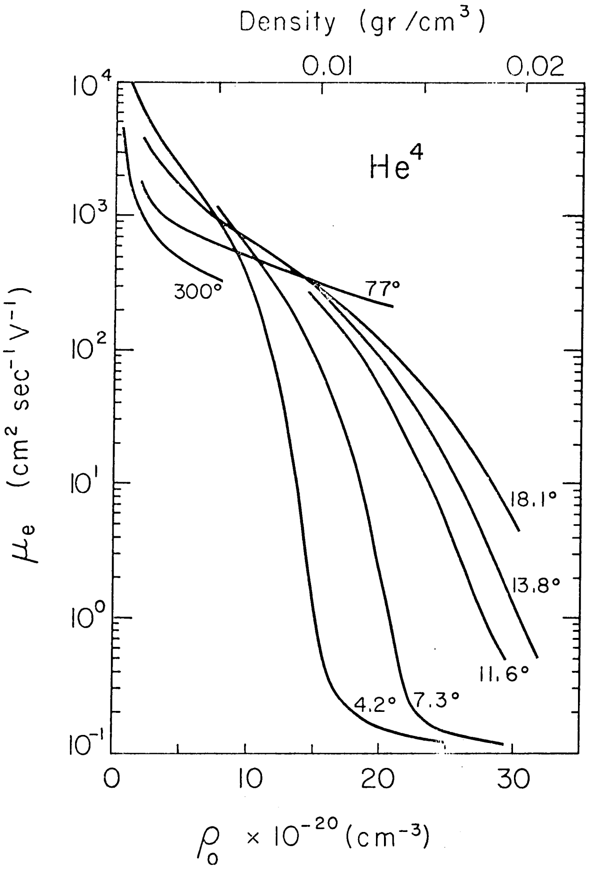

The only realistic possibility is then the one of using gas at suitable low density. From Fig. 2 one can see that bubbles exist only for $\rho > \rho_c$ and $T < T_c$ where ρ_c, T_c are determined by the free energy of the system. Taking $T \cong 4K$ we get $\rho > 1.2 \times 10^{21}\ cm^{-3}$ as a safe limit . This corresponds to $\rho \leq 10^{-2}\ gr/cm^3$, or about $\leq$ 15 times lower density than the liquid Helium or gas Helium at $\lesssim$ 44 atm and NPT.

Multiplication of the number of electron is then necessary before detection and thin wires at high voltage must run along the slots. A reasonable gain could be $\simeq 10^4$, leading to pulses about 100 times larger than the one from liquid Argon.

2. Sampling showers with gas counters. Expected resolutions

Estensive studies on calorimeters equipped with gas filled proportional counters have been performed by R.L. Anderson et al.[4]. Their main conclusions are as follows:

(1) the energy resolutions of shower counters have been investigated with electrons of 1,2,4,8 and 16 GeV. The resolution (s.deviation) is consistent with a law of the type:

$$\left.\frac{\Delta E}{E}\right|_{s.d.} = K/\sqrt{E}$$

with K = 0.185 (units are GeV). The calorimeter (Fig. 3) was made of 36 lead plates (0.423 r.ℓ) interleaved with 36 planes of multiwire planes 3/8'' wide. The resolution of a similar lead calorimeter but filled with liquid Argon built by Hitlin and coll.[4] is about 1.6 times better than the gas counters.

(2) A hadron calorimeter with iron plates was also built and tested. Plates were iron sheets about 3 cm thick, interspersed with gas counters (see Fig. 4). The instrument was tested with electrons and pions. The responses are characterized by a law:

$$\left.\frac{\Delta E}{E}\right|_{s.d.} = \frac{K}{\sqrt{E}} \qquad K/\sqrt{E}$$

with K = 0.44 for electrons and K = 0.72 for pions (all units are GeV). The best resolutions obtained by Willis and coll.[4] with liquid Argon have been K = 0.63 for iron plates and K = 0.316 for fission compensated uranium plates.

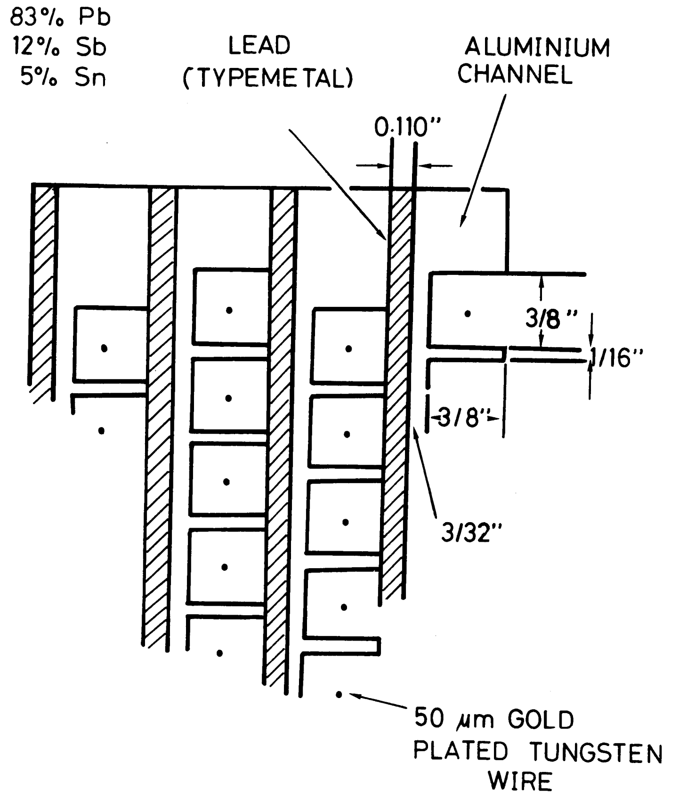

Fig. 3. DETAIL SECTION PWSC

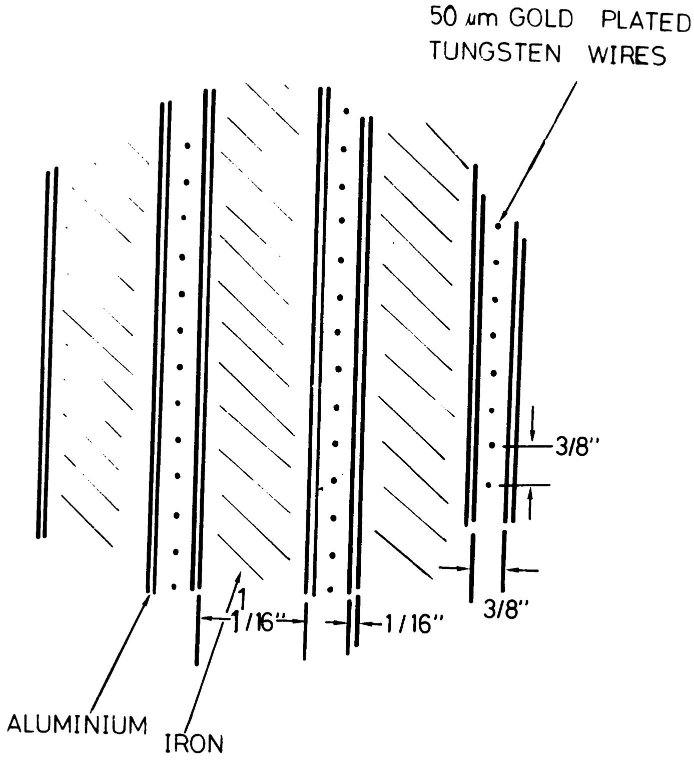

Fig. 4.
DETAIL SECTION HADRON CALORIMETER

(3) The major source of fluctuations in the energy measurement seems to be associated with the coarseness of the sampling. Taking every second (third) sampling increases resolution by a factor $\sqrt{2}$ ($\sqrt{3}$). Therefore a fission compensated calorimeter will not be appreciably better unless a much finer sampling is introduced.

In conclusion gas counters sample the energy depositions only slightly less accurately for hadrons and about a factor 1.6 time worse for e.m. showers.

3. A tentative dipole magnet-calorimeter configuration

The magnetic field is generated by a succession of cosθ current distributions. The shape of the current carrying superconducting wires is shown in Fig. 5. The basic formulae for the field and forces are given in Ref. 5. If we indicate with j the average current density in the point of maximum (y = 0) plate of thickness Δx increases the (uniform) field inside the cylinder by an amount:

$$\Delta B = 0.63 \;.\; j(A/mm^2) \;.\; \Delta x(m) \qquad \text{Tesla}$$

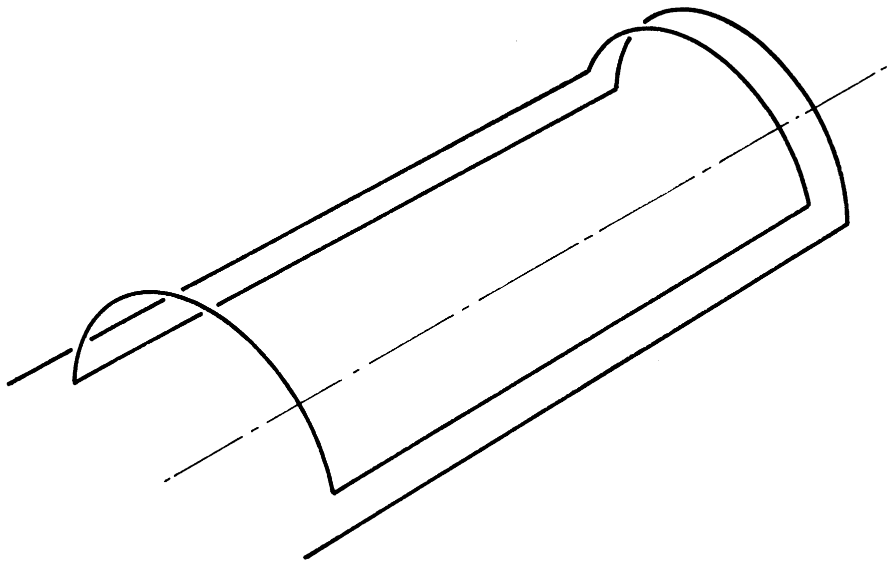

Fig. 5

For the reasonable thickness Δx = 3 cm and j = 10 A/mm² which is a safe value for a stabilised superconductor we get:

$$\Delta B = 0.20 \qquad \text{Tesla}$$

Note that this result is independent of the radius of the cylinder. In order to reach a central field value $B_o = 3$ Tesla, 15 concentric cylinders of this type are required. The force is equivalent to a pressure tending to push conductors apart and it has its maximum value in the equatorial plane:

$$P_{MAX} = B_o \, j \, . \, \Delta x \quad \text{(M.K.S.units)}$$

The innermost coil then at $B_o = 3T$ with $\Delta x = 0.03$ m and $j = 10 \times 10^6 A/m^2$ ($10 \; A/mm^2$) experiences a max. radial pressure of 9 Kg/cm^2. We can calculate the deformation of the plate using the formula derived in Appendix 1. The total force acting on half of the ring is 135 Ton/metre length and for a radius of 75 cm. The deformation of a free cylinder is then as large as $135 \times 10^3 \times 3.75 \times 10^{-5} = 5.06$ cm! Therefore the plates must be solidly connected with each other in order to discharge the mechanical pressures to the outside. The whole stack may be as thick as $15 \times 3 + 15 = 60$ cm and the total force is $135 \times \frac{15}{2} = 10^3$ Tons. Assuming a moment of inertia equals to 1/4 of the one of a solid steel block, one gets a deformation of 0.6 mm which is entirely acceptable. If not sufficient, additional straightening could be achieved by adding an additional external retaining cylinder.

Aknowledgements

Illuminating discussions with B. Willis and E. Fowler are greatly appreciated.

References

1) B. Willis and V. Radeky, NIM, 120, 221 (1974).

2) H.R. Harrison and B.E. Springett, Phys. Lett. 35A 73 (1971).

3) P.G. Lecomber et al., 'Solid State Communications', 18,377 (1976).

4) B.L. Anderson et al., PEP proposal PEP6.

5) C.W. Fabjan et al, submitted to NIM.

6) C. Rubbia, pp̄ Note 14, 1977.

Appendix 1

Deformation due to radial forces on a cylinder

Assume the idealized case of Fig. 1. A cylinder of length ℓ_o of average radius r_o and thickness h is subject to two diametrically opposite traction forces F. We shall determine the effects existing in s such a configuration.

We shall assume that the ring is ideally cut along the line indicated in Fig. 2. For symmetry reasons, no shear stress can exist along these sections. Instead we find a tension force F/2 and a bending moment M_o, which is defined in our case as positive if it tends to increase the local radius of the cylinder.

Along the section I defined by the polar angle ϕ (Fig. 2) we can calculate the internal forces and moments with the condition of equilibrium of the separate slices. Projecting the forces along N and T and calculating the bending moment along the section, we get (Fig. 2)

$$N = \frac{F}{2}\cos\phi \qquad T = \frac{F}{2}\sin\phi \tag{1}$$

$$M_f = M_o + \frac{F}{2} r (1 - \cos\phi)$$

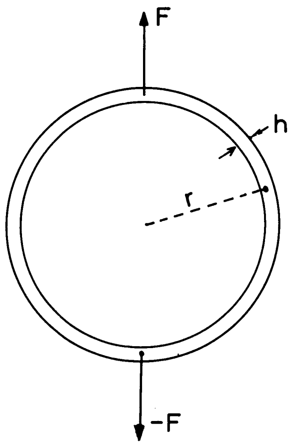

Fig. 1

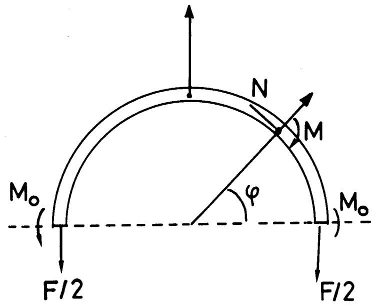

Fig.2

The work performed over the whole cylinder after the deformation is given by:

$$W = 4\int_0^{\pi/2}\left[\frac{1}{2ES}\left(N+\frac{M_f}{r}\right)^2+\frac{M_f^2}{2E\,I_o}+\frac{\chi T^2}{GS}\qquad r d\phi\right] \tag{2}$$

where:

E is the Young modulus

G is the modulus of rigidity

χ is a dimension less coefficient $\simeq$ 1.2 for rectangular cross-sections.

S is the moment of inertia. Its value is given by the formula:

I_o is the moment of inertia. Its value is given by the formula:

$$I_o = \left[Sr^2 \quad \frac{1}{12}\left(\frac{h}{r}\right)^2+\frac{1}{80}\left(\frac{h}{r}\right)^4+\frac{1}{448}\left(\frac{h}{r}\right)^6+\dots\dots\right]$$

for h < < r, the moment of inertia, given by the first term of the expansion coincides with the one of a rectangular section.

According to the theorem of Castigliano, the equilibrium conditions $\frac{\partial W}{\partial M_o}$ = 0, or equivalently to

$$\int_0^{\pi/2}\left[\frac{1}{ES}\left(N+\frac{M_f}{r}\right)\left(\frac{\partial N}{\partial M_o}+\frac{1}{r}\,\frac{\partial M_f}{\partial M_o}\right)+\right. \tag{3}$$

$$\left.+\quad\frac{M_f}{E\,I_o}\,\frac{\partial M_f}{\partial M_o}+\frac{\chi T}{GS}\,\frac{\partial T}{\partial M_o}\right]d\phi = 0$$

Setting $\frac{\partial N}{\partial M_o} = \frac{\partial T}{\partial M_o} = 0 \qquad \frac{\partial M_f}{\partial M_o} = 1,$ we get

$$\int_0^{\pi/2} \left\{ \frac{F\cos\phi}{2Sr} + \left(\frac{1}{Sr^2} + \frac{1}{I_o}\right)\left[M_o + \frac{Fr}{2}(1-\cos\phi)\right]\right\} d\phi = 0$$

Performing the integrals and solving respect to M_o we get:

$$M_o = - Fr\left(\frac{1}{2} - \frac{1}{\pi}\ \frac{Sr^2}{Sr^2 + I_o}\right) \tag{4a}$$

$$N_o = \frac{F}{2} \tag{4b}$$

For curvatures which are not too steep, i.e. $r >> \sqrt{\frac{I_o}{S}}$ we get

$$M_o \simeq - Fr\left(\frac{1}{2} - \frac{1}{\pi}\right)$$

To conclude, the total internal forces and moments are as a function of ϕ:

$$N = \frac{F}{2}\cos\phi \qquad\qquad T = \frac{F}{2}\sin\phi$$

$$M_f = \frac{Fr}{2}\left(\frac{2}{\pi}\ \frac{1}{1 + I_o/Sr^2} - \cos\phi\right) \tag{5}$$

Replacing the values of (5) in Eq. (2) integrating on ϕ we arrive at the following formula:

$$W = F^2 r\left[\frac{\pi^3}{64\ ES} + \frac{\pi r^2}{64\ I_o E}(\pi^2-6) + \frac{\pi}{32}\ \frac{\chi}{GS}\right] \tag{6}$$

In order to calculate the maximum sagitta we apply energy conservation and assuming that defractions are proportional to the applied force:

$$4 = \int F(s)ds = \frac{FS}{2} = W \qquad (7)$$

where S is the elongation of the radius of the cylinder. Combining (6) and (7) we get

$$S = \frac{\pi r F}{16}\left[\frac{\pi^2}{2ES} + (\pi^2-6)\frac{r^2}{2I_oE} + \frac{\chi}{GS}\right] \qquad (8)$$

For sufficiently large radii the second term is dominating and we get:

$$S \simeq \frac{(\pi^2-6)\ r^3F}{32\ I_oE} \simeq 0.121\frac{Fr^3}{I_oE}$$

which compares with the classic formula of a bar with a force at one end and fixed on the other side etc:

$$S = \frac{F\ell^3}{3I_oE}$$

Two formula coincide when $\ell = 1.40\ r \simeq \frac{\pi}{2}$ is as one would have expected.

Assume in one particular application a steel tube one metre long, of average radius of 75 cm and 20 cm thick. For steel we have $E = 2.1 \times 10^7\ Kg/cm^2$, $G = 0.77 \times 10^6\ Kg/cm^2$. The moment inertia is $I_o \cong 20 \times 100 \times (75)^2 \times \frac{1}{12}\left(\frac{2.0}{75}\right)^2 = 6.67 \times 10^4\ cm^4$. With these numbers we get:

$$\frac{S}{F} = 14.73\ (1.17 \times 10^{-10} + 7.76 \times 10^{-9} + 7.79 \times 10^{-10}) = 1.27 \times 10^{-7} cm/Kg$$

Note that the result goes like $\sim h^3$ and that a 3 cm thick sheet will give $\frac{S}{F} = 3.75 \times 10^{-5}$ cm/Kg.